10

Nuclear fusion

In this chapter we describe the nuclear reactions that power the Sun and thus make possible life on Earth. In contrast to the power from fission discussed in the preceding chapter, the radiance of the Sun comes from the fusion of the lightest element, hydrogen, into helium. We then examine the possibility of controlled nuclear fusion for power production on Earth.

10.1 The Sun

In stars, the gravitational, the weak, the electromagnetic, and the strong interactions all play an active and essential role. Our Sun and its planets are thought to have condensed out of a diffuse mass of material, mostly hydrogen and helium atoms, some 5×10^9 years ago. Table 10.1 gives the estimated proportions of the ten most abundant nuclei in that mass of material.

The major attributes of the Sun, determined from a wide variety of observations, are as follows:

Mass	$M_\odot = 1.99 \times 10^{30}$ kg
Radius	$R_\odot = 6.96 \times 10^8$ m
Luminosity	$L_\odot = 3.86 \times 10^{26}$ W.

(The luminosity of a star is the total rate of emission of electromagnetic energy.)

Because of the long range and universally attractive nature of gravity, a homogeneous mass of gas at sufficiently low temperature is unstable to contraction into objects like stars. During contraction of a mass of gas,

https://doi.org/10.1017/CBO9781139164405.013 Published online by Cambridge University Press

Table 10.1. *The proportion by number, relative to carbon, of the ten most abundant atoms in the Solar System at its birth*

H	He	C	N	O	Ne	Mg	Si	S	Fe
2400	162	1.0	0.21	1.66	0.23	0.10	0.09	0.05	0.08

Data from Cameron, A. G. W. (1992), in *Essays in Nuclear Astrophysics*, ed. C. A. Barnes, D. D. Clayton & D. N. Schramm. Cambridge University Press, p. 23.

gravitational potential energy is converted into kinetic energy and radiation energy, and the temperature of the gas rises. The rate of collapse is determined by the extent to which the build-up of pressure in the hot, dense interior can balance the incessant pressure of gravitational contraction. In a star like the Sun, as the temperature and density increased, its rate of contraction was essentially stopped when the interior became hot enough to ignite the hydrogen-burning reaction that we shall discuss in detail presently. At this stage in the Sun's evolution, the generated nuclear power keeps the interior hot enough to sustain the pressure that balances gravity, and a quasi-static condition is established, a condition that exists today. This condition is not one of thermodynamic equilibrium, since the interior is hotter than the outside and the nuclear energy liberated at the centre is transferred, radiatively and by conduction and convection, to the surface, where it is radiated out into space, to our benefit, and gives the Sun its luminosity.

The principal reactions that power the Sun begin with the conversion of hydrogen into deuterium:

$$\mathrm{p} + \mathrm{p} \rightarrow {}^{2}_{1}\mathrm{H} + \mathrm{e}^{+} + \nu_{\mathrm{e}} + 0.42\ \mathrm{MeV}. \tag{10.1}$$

This reaction involves the weak interaction (a proton changes to a neutron), and so occurs very rarely. It is the weak interaction that sets the long time scale of the quasi-static state of the Sun.

The positron produced in the reaction quickly annihilates with an electron to release a further 1.02 MeV of energy. The deuterium is converted to ^{3}He:

$$\mathrm{p} + {}^{2}_{1}\mathrm{H} \rightarrow {}^{3}_{2}\mathrm{He} + \gamma + 5.49\ \mathrm{MeV}, \tag{10.2}$$

which in turn fuses to ^{4}He:

https://doi.org/10.1017/CBO9781139164405.013 Published online by Cambridge University Press

$$^3_2\mathrm{He} + {}^3_2\mathrm{He} \rightarrow {}^4_2\mathrm{He} + \mathrm{p} + \mathrm{p} + 12.86\ \mathrm{MeV}. \tag{10.3}$$

Thus the net result of these reactions, which are called the 'PPI chain', is the conversion of hydrogen to helium with an energy release of 26.73 MeV per helium nucleus formed. The neutrinos emitted in the p–p reactions take an average 0.26 MeV of energy each. This energy is lost into outer space, but is not included in the observed luminosity. Thus each hydrogen atom consumed in this process leads to the emission of 6.55 MeV of electromagnetic energy from the Sun.

The observed solar luminosity implies that $L_\odot/(6.55\ \mathrm{MeV}) = 3.7 \times 10^{38}$ hydrogen atoms are converted into helium per second. This rate of conversion, over the lifetime of the Sun, gives a total of 5.4×10^{55} conversions. The Sun's mass and composition show that it started with about 8.9×10^{56} hydrogen atoms. We can conclude that less than 10% of the hydrogen of the Sun has so far been consumed, and appreciate the long time scale of this stage of stellar evolution.

Figure 10.1 shows the density, temperature and thermonuclear-power density from a model calculation of the Sun as it is now. It it interesting to note that 50% of the mass is within a distance of $R_\odot/4$ from the centre, and 95% of the luminosity is produced in the central region within a distance of $R_\odot/5$, where the temperature is such that $k_\mathrm{B}T \gtrsim 1$ keV. (k_B is Boltzmann's constant and $k_\mathrm{B}T = 1$ keV when $T = 1.16 \times 10^7$ K.)

A simple order-of-magnitude calculation shows that the gravitational energy released in contraction, before the quasi-static period began, is sufficient to produce such temperatures:

$$\text{gravitational energy } \sim \frac{GM_\odot^2}{R_\odot} = 3.8 \times 10^{41}\ \mathrm{J},$$

where the gravitational constant $G = 6.67 \times 10^{-11}\ \mathrm{m^3\ kg^{-1}\ s^{-2}}$. This energy would give ~ 1 keV of kinetic energy on average to every particle, nuclei and electrons. At these temperatures the hydrogen and helium atoms will be completely ionised; material in this condition is known as *plasma*.

10.2 Cross-sections for hydrogen burning

We turn now to a more-detailed examination of the nuclear physics involved in hydrogen burning. Reactions involving charged particles were discussed in §8.3, where the role of the Coulomb barrier was empha-

https://doi.org/10.1017/CBO9781139164405.013 Published online by Cambridge University Press

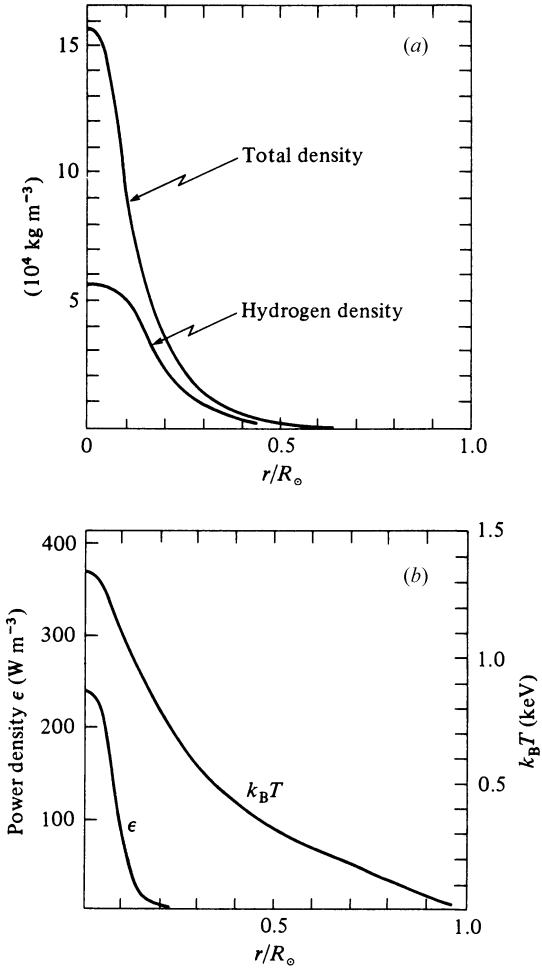


Fig. 10.1 (*a*) Mass densities and (*b*) the thermonuclear power density ε and the temperature T, in the modern Sun as a function of distance r from the centre. (Taken from model calculations by Bahcall, J. N. *et al.* (1982), *Rev. Mod. Phys.* **54**, 767.)

sised. For energies in the range of keV we shall use the low-energy expression for charged-particle reactions given by equation (8.7):

$$\sigma(E) = \frac{1}{E} S(0) \mathrm{e}^{-\sqrt{(E_G/E)}} \tag{10.4}$$

where

https://doi.org/10.1017/CBO9781139164405.013 Published online by Cambridge University Press

$$E_G = 2mc^2\left(\frac{\pi Z_1 Z_2 e^2}{\hbar c(4\pi\varepsilon_0)}\right)^2.$$

A more accurate expression may be necessary if there is a resonance in the keV energy range.

Direct measurements of the cross-sections of reactions (10.2) and (10.3) at energies of 1 keV have not been made since they are so small, but values of $S(0)$ are known by extrapolation from measurements at higher energies. The p–d reaction (10.2) has been measured down to 15 keV and $S_{\mathrm{pd}}(0) \approx 2.5 \times 10^{-7}$ MeV b. The helium–helium reaction (10.3) has been measured down to 33 keV, giving $S_{\mathrm{hh}}(0) \approx 4.7$ MeV b. The p–d cross-section is small because it necessarily involves a γ-transition to satisfy both energy and momentum conservation. The p–p reaction (10.1), the first stage of hydrogen burning, has a cross-section which is lower by many orders of magnitude because it involves the weak interaction. Although the reaction is crucial, the cross-section is so small that it has not been directly measured in a laboratory at any energy. Fortunately we have such a precise theory of the weak interaction that the cross-section, and $S_{\mathrm{pp}}(0)$, can be calculated with some confidence; it is found that

$$S_{\mathrm{pp}}(0) \approx 3.88 \times 10^{-25}\ \mathrm{MeV\,b}. \tag{10.5}$$

This order of magnitude is not too difficult to understand. As is explained in Chapter 3, the proton–proton nuclear potential has been determined from scattering experiments. From the potential, the low-energy proton–proton nuclear-scattering cross-section can be calculated. Although there is no resonance, the nuclear attraction makes the cross-section quite large, 36 barns, at energies $\gtrsim 1$ MeV which are low but are above the Coulomb barrier. Reaction (10.1) involves the protons coming together within the range of the nuclear force (Fig. 3.2) and, while they are together, a β-decay taking place. We can estimate the probability of this β-decay by

$$\text{probability} = \frac{\text{a typical nuclear time}}{\text{a } \beta\text{-decay time}}.$$

Consider the cross-section at 1 MeV. Since the energy released in the reaction is comparable with the energy released in the β-decay of a free neutron, it is reasonable to take the β-decay time to be the neutron lifetime, 887 s, and the nuclear time is $\sim 10^{23}$ s (§5.2). The cross-section for

https://doi.org/10.1017/CBO9781139164405.013 Published online by Cambridge University Press

the proton–proton to deuteron reaction at 1 MeV should thus be of the order

$$\sigma \sim (36\ \text{b}) \times \left(\frac{10^{-23}\ \text{s}}{887\ \text{s}}\right) = 4 \times 10^{-25}\ \text{b}.$$

Since the energy of 1 MeV is above the Coulomb barrier, we can infer that $S_{\text{pp}} \sim 4 \times 10^{-25}$ MeV b. This excellent agreement with equation (10.5) is fortuitous, but the argument does make intelligible the order of magnitude of this key quantity.

10.3 Nuclear reaction rates in a plasma

During the early cold stages of stellar contraction, nuclei do not have kinetic energies high enough, compared with the Coulomb barriers between them, for the barrier penetration probability to be significant. To obtain the reaction rate for a process in the interior of a star and see how it depends on temperature, we must average suitably over the energies of the particles involved. The calculation is an important one so we shall set it out here.

Consider the nuclei in a volume of plasma small enough for the temperature and number densities to be considered uniform. We shall assume that the velocities of the nuclei are given by the Maxwell–Boltzmann distribution, so that the probability of two nuclei having a relative velocity v in the range, v, $v + \mathrm{d}v$ is given by

$$P(v)\mathrm{d}v = \left(\frac{2}{\pi}\right)^{\frac{1}{2}} \left(\frac{m}{k_{\text{B}}T}\right)^{\frac{3}{2}} \mathrm{e}^{-mv^2/2k_{\text{B}}T} v^2 \mathrm{d}v,$$

where m is the reduced mass of the pair. (The centre-of-mass motion has been factored out.)

If the nuclei are labelled by a, b, with number densities ρ_a, ρ_b, the number of reactions per unit time per unit volume is

$$\text{reaction rate per unit volume} = K\rho_a\rho_b(\overline{v\sigma_{ab}}), \tag{10.6}$$

where σ_{ab} is the cross-section for the reaction, and the bar denotes the average over the velocity distribution. Equation (10.6) follows from the discussion of reaction rates in Appendix A. The factor $K = 1$ if the nuclei are different and $K = \frac{1}{2}$ if the nuclei are the same.

https://doi.org/10.1017/CBO9781139164405.013 Published online by Cambridge University Press

We have

$$\overline{v\sigma_{ab}} = \int_0^\infty v\sigma_{ab} P(v)\mathrm{d}v.$$

Changing variables to $E = mv^2/2$, and using the low-energy formula (10.4) for the cross-section, this becomes

$$\overline{v\sigma_{ab}} = \left(\frac{8}{\pi m}\right)^{\frac{1}{2}} \left(\frac{1}{k_\mathrm{B}T}\right)^{\frac{3}{2}} S_{ab}(0) \int_0^\infty \mathrm{e}^{-\phi(E)}\mathrm{d}E, \tag{10.7}$$

where $\phi(E) = E/k_\mathrm{B}T + \sqrt{(E_G/E)}$.

The function $\mathrm{e}^{-\phi(E)}$ is sharply peaked. It falls off rapidly at high energies because of the Boltzmann factor, and at low energies because of the barrier-penetration factor. The peak lies at $E = E_0$ where $\phi(E)$ is a minimum, i.e. where $\mathrm{d}\phi/\mathrm{d}E = 0$, which gives

$$E_0 = (E_G)^{\frac{1}{3}}(k_\mathrm{B}T/2)^{\frac{2}{3}}.$$

Figure 10.2 is a graph of $\mathrm{e}^{-\phi(E)}$ appropriate to the p–p reaction at the centre of the Sun.

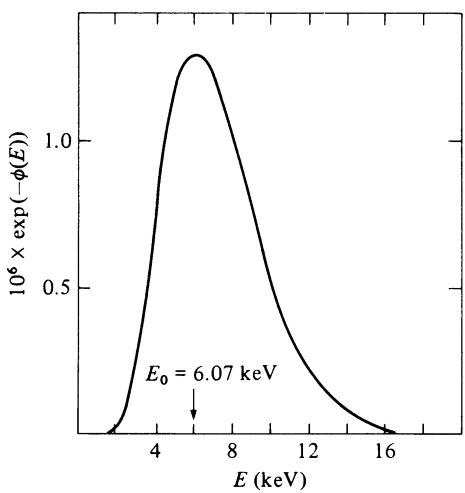


Fig. 10.2 The function $\exp(-\phi(E))$ appearing in equation (10.7), plotted for the proton–proton reaction at $k_\mathrm{B}T = 1.34$ keV.

https://doi.org/10.1017/CBO9781139164405.013 Published online by Cambridge University Press

As it stands, the integral cannot be performed analytically, but the main contribution comes from the peak. It is possible to replace $\phi(E)$ in the neighbourhood of E_0 by a simpler expression, leading to an analytic result for the integral (which is also a good approximation). The Taylor expansion of $\phi(E)$ about E_0 gives

$$\phi(E) \approx \phi(E_0) + \tfrac{1}{2}(E - E_0)^2 \phi''(E_0),$$

where

$$\phi(E_0) = 3(\tfrac{1}{2})^{\frac{2}{3}}(E_G/k_\mathrm{B}T)^{\frac{1}{3}},$$
$$\phi''(E_0), = 3(\tfrac{1}{2})^{\frac{1}{3}}E_G^{-\frac{1}{3}}(k_\mathrm{B}T)^{-\frac{5}{3}}.$$

The linear term does not appear, since $\phi'(E_0) = 0$. With this approximation, the integrand is replaced by a Gaussian peak and the integration range can be extended down to $E = -\infty$ with negligible error. We have then, remembering the result $\int_{-\infty}^{\infty} \mathrm{e}^{-ax^2}\mathrm{d}x = (\pi/a)^{\frac{1}{2}}$, the fairly simple expression

$$\overline{v\sigma_{ab}} = \tfrac{8}{9}S_{ab}(0)\left(\frac{2}{3mE_G}\right)^{\frac{1}{2}}\tau^2\mathrm{e}^{-\tau}$$

with

$$\tau = 3(\tfrac{1}{2})^{\frac{2}{3}}(E_G/k_\mathrm{B}T)^{\frac{1}{3}} = 3\left(\frac{mc^2}{2k_\mathrm{B}T}\right)^{\frac{1}{3}}\left(\frac{\pi Z_a Z_b e^2}{\hbar c(4\pi\varepsilon_0)}\right)^{\frac{2}{3}}. \tag{10.8}$$

For practical calculations, taking the masses of nuclei to be $A\times$ (one atomic mass unit) gives

$$\overline{v\sigma_{ab}} = \frac{7.21\times10^{-22}}{Z_aZ_b}\frac{(A_a + A_b)}{A_aA_b}\left(\frac{S_{ab}(0)}{1\ \mathrm{MeV\ b}}\right)\tau^2\mathrm{e}^{-\tau}\ \mathrm{m}^3\ \mathrm{s}^{-1},$$

and

$$\tau = 18.8\left(\frac{Z_a^2Z_b^2A_aA_b}{A_a + A_b}\right)^{\frac{1}{3}}\left(\frac{1\ \mathrm{keV}}{k_\mathrm{B}T}\right)^{\frac{1}{3}}.$$

https://doi.org/10.1017/CBO9781139164405.013 Published online by Cambridge University Press

Note that the temperature dependence of $\overline{v\sigma}$ lies entirely in the factor $\tau^2 e^{-\tau}$.

The temperature dependence is dramatic, as also is the dependence on the nuclear species involved. Both are illustrated in Fig. 10.3, which shows plots of $\tau^2 e^{-\tau}$ against temperature for several reactions of astrophysical interest. Note that the vertical scale extends over a range of 10^{60}!

For a given set of nuclear reactions, we can write down equations giving the rate of change of the number densities ρ of the nuclei participating, in a region of given temperature. For example, considering the PPI reactions and writing $\lambda_{ab} = \overline{v\sigma_{ab}}$, we have, from reactions (10.1) and (10.2) and equation (10.6),

$$\frac{\partial \rho_d}{\partial t} = \tfrac{1}{2}\lambda_{pp}\rho_p^2 - \lambda_{pd}\rho_p\rho_d.$$

Because of the long time scale of hydrogen burn-up, ρ_p may be regarded as constant in this equation, giving the solution

$$\rho_d(t) = (\tfrac{1}{2}\lambda_{pp}/\lambda_{pd})\rho_p(1 + Ce^{-\lambda_{pd}\rho_p t}),$$

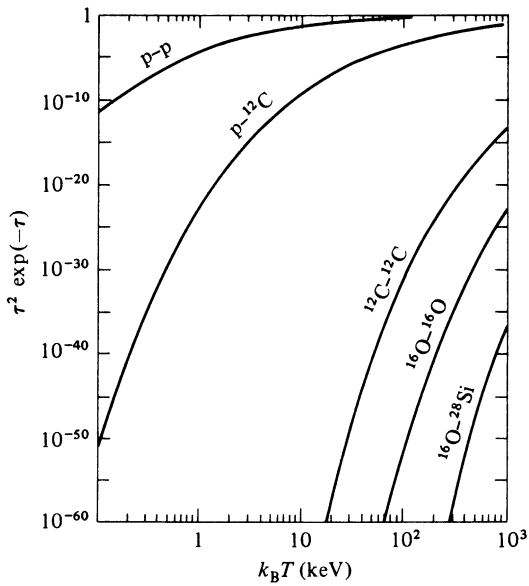


Fig. 10.3 The function $\tau^2 \exp(-\tau)$ appearing in equation (10.8), for some nuclear reactions.

https://doi.org/10.1017/CBO9781139164405.013 Published online by Cambridge University Press

where C is a constant.

Using the numerical values for $S_{pp}(0)$ given in §10.2, and a temperature and density appropriate to the centre of the Sun, from Fig. 10.1, we find that the time constant for establishing equilibrium is $(\lambda_{pd}\rho_p)^{-1} = 3.3$ s. Thus our assumption that ρ_p could be treated as a constant was valid. In equilibrium, the ratio $\rho_d/\rho_p = \frac{1}{2}\lambda_{pp}/\lambda_{pd} = 1.5 \times 10^{-18}$. The low density of deuterium accounts for our neglect of d–d reactions (which are considered in §10.6).

10.4 Other solar reactions

Our account above of hydrogen burning in the Sun is not complete. There are other ways of consuming the ^{3}He formed in reaction (10.2). The presence of ^{4}He in a star leads to the formation of ^{7}Be:

$$^3_2\mathrm{He} + {}^4_2\mathrm{He} \rightarrow {}^7_4\mathrm{Be} + \gamma + 1.59\ \mathrm{MeV}. \tag{10.9}$$

^{7}Be is unstable to the capture of a free electron from the plasma to form ^{7}Li:

$$^7_4\mathrm{Be} + \mathrm{e}^- \rightarrow {}^7_3\mathrm{Li} + \nu_\mathrm{e} + 0.86\ \mathrm{MeV}, \tag{10.10a}$$

or, with 10.3% probability, to form an excited state $^7_3$Li*:

$$^7_4\mathrm{Be} + \mathrm{e}^- \rightarrow {}^7_3\mathrm{Li}^* + \nu_\mathrm{e} + 0.38\ \mathrm{MeV}, \tag{10.10b}$$

which then decays:

$$^7_3\mathrm{Li}^* \rightarrow {}^7_3\mathrm{Li} + \gamma + 0.48\ \mathrm{MeV}.$$

$^7_3$Li is quickly broken up by a proton into two helium nuclei:

$$^7_3\mathrm{Li} + \mathrm{p} \rightarrow {}^4_2\mathrm{He} + {}^4_2\mathrm{He} + 17.35\ \mathrm{MeV}. \tag{10.11}$$

These reactions form the 'PPII chain'.

Alternatively, the $^7_4$Be may interact with a proton to form $^8_5$B:

$$^7_4\mathrm{Be} + \mathrm{p} \rightarrow {}^8_5\mathrm{B} + \gamma + 0.14\ \mathrm{MeV}. \tag{10.12}$$

$^8_5$B is unstable to β-decay,

https://doi.org/10.1017/CBO9781139164405.013 Published online by Cambridge University Press

$$^{8}_{5}\mathrm{B} \rightarrow {}^{8}_{4}\mathrm{Be}^{*} + \mathrm{e}^{+} + \nu_{\mathrm{e}} + 14.02\ \mathrm{MeV}, \tag{10.13}$$

and $^{8}_{4}\mathrm{Be}^{*}$ breaks up into two helium nuclei:

$$^{8}_{4}\mathrm{Be}^{*} \rightarrow {}^{4}_{2}\mathrm{He} + {}^{4}_{2}\mathrm{He} + 3.03\ \mathrm{MeV}; \tag{10.14}$$

this is the 'PPIII chain'. The positron annihilates with an electron to release a further 1.02 MeV.

The relative importance of the PPII and PPIII chains, compared with the PPI chain, can be calculated from the appropriate set of rate equations; in the standard model of the Sun, the PPI chain is the main process.

Another interesting set of reactions resulting in the burning of hydrogen to helium is the 'CNO' cycle. The presence of any of the nuclei $^{12}_{6}\mathrm{C}$, $^{13}_{6}\mathrm{C}$, $^{14}_{7}\mathrm{N}$ or $^{15}_{7}\mathrm{N}$ catalyses the burning by the set of reactions

$$\begin{aligned} &^{12}\mathrm{C} + \mathrm{p} \rightarrow {}^{13}\mathrm{N} + \gamma, \quad {}^{13}\mathrm{N} \rightarrow {}^{13}\mathrm{C} + \mathrm{e}^{+} + \nu_{\mathrm{e}} \\ &^{13}\mathrm{C} + \mathrm{p} \rightarrow {}^{14}\mathrm{N} + \gamma \\ &^{14}\mathrm{N} + \mathrm{p} \rightarrow {}^{15}\mathrm{O} + \gamma, \quad {}^{15}\mathrm{O} \rightarrow {}^{15}\mathrm{N} + \mathrm{e}^{+} + \nu_{\mathrm{e}} \\ &^{15}\mathrm{N} + \mathrm{p} \rightarrow {}^{12}\mathrm{C} + {}^{4}\mathrm{He}. \end{aligned} \tag{10.15}$$

The weak interactions in the cycle are not compelled to occur in a fleeting 10^{-23} s, as in the p–p reaction, but can proceed at their leisure in the usual β-decay times. Carbon and nitrogen nuclei are known to be present in the Sun (Table 10.1), but at the temperatures of the Sun the reaction rates are greatly suppressed by the Coulomb barrier (Fig. 10.3), and the CNO cycle probably accounts for only about 3% of stellar hydrogen burning. In hotter stars the CNO cycle may dominate over the PP chains, since the CNO cycle reaction rates increase more rapidly with temperature (Fig. 10.3 again).

10.5 Solar neutrinos

The solar reactions described in §10.1 and §10.4 lead to a considerable flux of neutrinos through the Earth. The flux spectra predicted by the standard solar model are shown in Fig. 10.4. The band spectra result when the neutrino is produced with an accompanying positron. For example, pp refers to the process described by equation (10.1). Line spectra result when there is no accompanying positron to share the energy release.

https://doi.org/10.1017/CBO9781139164405.013 Published online by Cambridge University Press

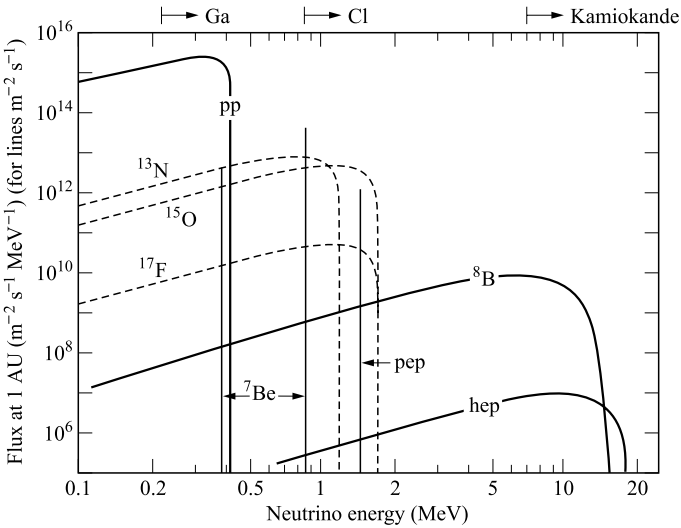


Fig. 10.4 The solar neutrino spectra predicted by the standard solar model. Spectra for the pp chain are shown by solid lines and those for the CNO chain by dashed lines. (See Bahcall, J. N. and Ulrich, R. K. (1988), *Rev. Mod. Phys.* **60**, 297.)

The line spectra marked ^{7}Be come from the processes (10.10a) and (10.10b). The pep line is from the three-body reaction

$$\mathrm{p} + \mathrm{e}^{-} + \mathrm{p} \rightarrow {}^{2}_{1}\mathrm{H} + \nu_{\mathrm{e}} + 1.44\ \mathrm{MeV}. \tag{10.16}$$

This is a very rare alternative to the process (10.1). Almost all of the 1.44 MeV released is taken by the neutrino and so does not serve to heat the plasma. The hep spectrum comes from another very rare reaction, converting $^{3}_{2}$He into $^{4}_{2}$He:

$$\mathrm{p} + {}^{3}_{2}\mathrm{He} \rightarrow {}^{4}_{2}\mathrm{He} + \mathrm{e}^{+} + \nu_{\mathrm{e}} + 18.77\ \mathrm{MeV}. \tag{10.17}$$

This is an alternative to the main mechanism given by equation (10.3).

The cross-sections for neutrino interactions are so small that solar neutrinos arrive at the Earth more or less directly from the thermonuclear furnace at the Sun's core. Measurements of the solar neutrino spectrum provide a valuable check on our understanding of the Sun, and in fact the measurements have also provided valuable information on the nature of neutrinos themselves.

https://doi.org/10.1017/CBO9781139164405.013 Published online by Cambridge University Press

Two basic techniques have been employed, that cover different regions of the spectrum. The lowest energies are probed through the neutrino reaction

$$\nu_e + {}^{71}_{31}\mathrm{Ga} + 0.23\ \mathrm{MeV} \rightarrow {}^{71}_{32}\mathrm{Ge} + e^- . \tag{10.18}$$

As can be seen from Fig. 10.4, over 99% of all the solar neutrinos in the energy range from the threshold energy for the reaction, 0.23 MeV, up to a maximum energy of 0.42 MeV, come from the basic pp reaction (10.1). Only the gallium experiments cover this low-energy region.

Although low-energy solar neutrinos are copious, their interaction cross-section is particularly small (see §13.1). At the GALLEX experiment in Italy, 30 tons of gallium in a $GaCl_3$–HCl solution serves as target. The germanium produced binds chemically to form the volatile molecule $GeCl_4$, which is collected in the vapour above the liquid. The production rate of germanium (a few molecules per day) is determined by observing the characteristic Auger electrons and X-rays emitted in the K-capture decays of ^{71}Ge:

$$ {}^{71}_{32}\mathrm{Ge} + e^- \rightarrow {}^{71}_{31}\mathrm{Ga} + \nu_e .$$

At the Homestake Mine experiment in the USA, the neutrino flux is measured through the reaction

$$\nu_e + {}^{37}_{17}\mathrm{Cl} + 0.81\ \mathrm{MeV} \rightarrow e^- + {}^{37}_{18}\mathrm{Ar}. \tag{10.19}$$

The detector in this experiment consists of 615 tons of liquid perchloroethylene, C_2Cl_4. (The natural abundance of ^{37}Cl is 24%.) The argon produced in the experiment is extracted, and measured by monitoring its decay by K-capture, in a similar way to the gallium experiment. The threshold energy of 0.81 MeV makes the ^{37}Cl detector blind to the neutrinos from the pp reaction. The detector is particularly sensitive to high-energy neutrinos from the ^{8}B decay of equation (10.13).

An entirely different technique is used at the SuperKamiokande detector in Japan. This looks for elastic scattering of solar neutrinos from electrons in the target:

$$\nu_e + e^- \rightarrow \nu_e' + e^{-'} .$$

https://doi.org/10.1017/CBO9781139164405.013 Published online by Cambridge University Press

The target is ~ 20 kilotonnes of very pure water, H_2O. In many materials, the atomic nuclei have large cross-sections for electron production through reactions like (10.18) or (10.19). However, in the case of H_2O there is no such reaction for a proton, and the threshold energy for electron production from ${}^{16}_{8}\mathrm{O}$ (the principal 99.7% stable isotope of oxygen) is 14.9 MeV – too high for all but a few solar neutrinos. Elastic scattering from the electrons is thus the dominant reaction of solar neutrinos in water.

The water acts not only as target but also as detector. The scattered electrons emit Cerenkov light, which is registered by photomultipliers. To reduce background, counting is restricted to electrons with a recoil energy greater than about 7 MeV. Hence the detector is sensitive only to ${}^{8}\mathrm{B}$ and hep neutrinos.

The Cerenkov radiation gives information on the scattered electron's direction, which is close to that of the incident neutrino. This directional capacity makes water detectors more discriminating instruments than gallium or chlorine detectors. Water detectors can also time individual events. We shall see significant applications of timing in §11.4.

For all neutrinos, event rates are necessarily very low, of the order of one per day, and much patience is required to build up a significant data set. However, after several years accumulating data, all detectors tell a consistent and significant story: over the whole spectrum the event rate is about one-half the expected rate. It is not thought that this discrepancy is the result of our misunderstanding of the Sun, but that it is due to the nature of neutrinos themselves. We reserve until Chapter 13 the explanations and implications of these observations.

10.6 Fusion reactors

For the generation of nuclear fusion power on Earth the immeasurably slow p–p reaction is useless. However, Coulomb barriers for the deuteron, ${}^{2}_{1}\mathrm{H}$, are the same as for the proton, and the exothermic reactions

$$\begin{aligned} {}^{2}_{1}\mathrm{H} + {}^{2}_{1}\mathrm{H} &\rightarrow {}^{3}_{2}\mathrm{He} + \mathrm{n} + 3.27\ \mathrm{MeV}, \\ {}^{2}_{1}\mathrm{H} + {}^{2}_{1}\mathrm{H} &\rightarrow {}^{3}_{1}\mathrm{H} + \mathrm{p} + 4.03\ \mathrm{MeV}, \end{aligned} \tag{10.20}$$

suggest deuterium to be a suitable fuel for a fusion power station. The natural abundance of deuterium is large, 0.015% of all hydrogen, and

https://doi.org/10.1017/CBO9781139164405.013 Published online by Cambridge University Press

supplies of deuterium, in sea water for example, are effectively unlimited. The mass ratio of 2:1 makes isotope separation relatively easy.

Current research is more concerned with deuterium–tritium mixtures as fuel, using the reaction

$$^{2}_{1}\mathrm{H} + {}^{3}_{1}\mathrm{H} \rightarrow {}^{4}_{2}\mathrm{He} + \mathrm{n} + 17.62\ \mathrm{MeV}. \tag{10.21}$$

This has two advantages over the reactions (10.20). First, the heat of reaction is greater. Second, and more important, the cross-section is considerably larger (Fig. 10.5), because of an excited state of $^{5}_{2}$He which gives a resonance in the cross-section. The principal disadvantage is that tritium, $^{3}_{1}$H, must be manufactured; it has no natural abundance since it undergoes β-decay with a mean life of 17.7 years. As Fig. 10.5 shows, the peak of $\overline{v\sigma}$ is at $k_{\mathrm{B}}T = 60$ keV, and a temperature of 20 keV is regarded as a practical working temperature by fusion researchers.

A plasma at a temperature of 20 keV will vaporise any material container with which it comes into contact; current projects generally involve pulsed devices which contain and heat the plasma for short bursts of time only. For example, the moving electrically charged particles of the plasma may be confined for short times, and even compressed, by magnetic fields,

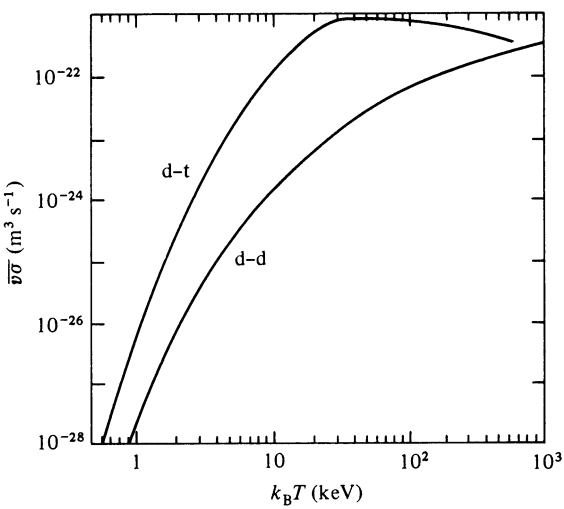


Fig. 10.5 Values of $(\overline{v\sigma})$ (see equation (10.7) for the combined deuterium–deuterium reactions (10.20) and the deuterium–tritium reaction (10.21). (Data from Keefe, D. (1982), *Ann. Rev. Nucl. Part. Sci.* **32**, 391.)

https://doi.org/10.1017/CBO9781139164405.013 Published online by Cambridge University Press

and heated by electromagnetic fields. Instruments such as the Joint European Torus (JET) at Culham are investigating these possibilities.

Inertial confinement, by the implosion of small pellets containing the deuterium–tritium fuel mixture, with the energy for implosion provided by pulsed laser beams, is another active area of research. A continuing series of 'mini-explosions' of such pellets, each containing a few milligrams of fuel, is envisaged. The scenario for such a reactor usually includes lithium in the heat-exchange blanket, since this provides a way of breeding tritium through the reactions

$$^{7}\mathrm{Li} + \mathrm{n} + 2.46\,\mathrm{MeV} \rightarrow {}^{3}\mathrm{H} + \alpha + \mathrm{n},$$
$$^{6}\mathrm{Li} + \mathrm{n} \rightarrow {}^{3}\mathrm{H} + \alpha + 48\ \mathrm{MeV}.$$

(The natural abundances of ^{6}Li and ^{7}Li are 7.4% and 92.6% respectively.) The endothermic first reaction can be brought about by the fast neutrons produced in the deuterium–tritium reaction, and it is clear that in principle a breeding ratio of greater than one is possible.

To achieve a temperature T in a deuterium–tritium plasma there must be an energy input to the plasma of $4\rho_{\mathrm{d}}(3k_{\mathrm{B}}T/2)$ per unit volume, where ρ_{d} is the number density of deuterium ions and of tritium ions (i.e. $\rho_{\mathrm{t}} = \rho_{\mathrm{d}}$, and the electron density is $2\rho_{\mathrm{d}}$, giving $4\rho_{\mathrm{d}}$ particles per unit volume). The reaction rate in the plasma is $\rho_{\mathrm{d}}^{2}\overline{\sigma v}$. If the plasma is confined for a time t_{c} then, per unit volume of plasma,

$$\frac{\text{fusion energy output}}{\text{energy intput}} = \frac{\rho_{\mathrm{d}}^{2}\overline{\sigma v}t_{\mathrm{c}}(17.6\ \mathrm{MeV})}{6\rho_{\mathrm{d}}k_{\mathrm{B}}T} \approx (10^{-19}\ \mathrm{m}^{3}\ \mathrm{s}^{-1})\rho_{\mathrm{d}}t_{\mathrm{c}}, \tag{10.22}$$

evaluating the right-hand side at $k_{\mathrm{B}}T = 20$ keV with the help of Fig. 10.5.

The plasma heating is certainly inefficient, so that a substantial fraction of useful energy is lost in this process, and the conversion of fusion energy to electricity is also (necessarily) inefficient. Hence a requirement for a useful device is that (fusion energy output)/(energy input) > 1, say. From equation (10.22), this is equivalent to the criterion $\rho_{\mathrm{d}}t_{\mathrm{c}} > 10^{19}\ \mathrm{m}^{-3}$ s. This is known as the *Lawson criterion*. More stringent formulations can be constructed for particular devices.

It should be appreciated that the engineering problems associated with either magnetic or inertial confinement as a basis for a working power station are immense and have not so far been solved in practice.

https://doi.org/10.1017/CBO9781139164405.013 Published online by Cambridge University Press

The Lawson criterion provides an estimate of how close a particular design is to achieving practical results.

10.7 Muon-catalysed fusion

To end this chapter, we shall describe *muon-catalysed fusion*. This process is experimentally well established, and quite well understood theoretically. The most interesting case, with power production in mind, is that of muons incident on a dense mixture of deuterium D_2 and tritium T_2 molecules.

Muons result from the predominant mode of decay of negative pions (see Fig. 3.5):

$$\pi^- \rightarrow \mu + \bar{\nu}_\mu .$$

The mean life of a charged pion is 2.60×10^{-8} s. The muon also decays through the weak interaction (see §2.5):

$$\mu \rightarrow \nu_\mu + e^- + \bar{\nu}_e ,$$

but it has a much longer mean life of 2.2×10^{-6} s. Thus a beam of negative pions is rapidly converted into a beam made up almost entirely of muons. Pions are produced in nuclear reactions when particles accelerated to high energy interact with target nuclei. The energy cost of producing muons by this route is estimated to be ~ 5 GeV per muon (very much greater than the rest mass energy of the muon ~ 106 MeV).

The atomic and molecular physics of nuclei and muons is very similar to that of nuclei and electrons, except for differences in scale. To a first approximation, binding energies scale by the mass ratio $(m_\mu/m_e) \approx 207$, and distances scale by $(m_e/m_\mu) \approx 1/207$. The characteristic energy unit of atomic and molecular physics, 1 Rydberg $= m_e(e^2/4\pi\varepsilon_0)^2/2\hbar^2 = 13.6$ eV, is replaced by its muonic equivalent,

$$m_\mu(e^2/4\pi\varepsilon_0)^2/2\hbar^2 = 2.81 \text{ keV}.$$

The Bohr radius, $a_0 = (4\pi\varepsilon_0)\hbar^2/m_e e^2 = 0.529$ Å is replaced by the muonic Bohr radius,

$$a_\mu = (4\pi\varepsilon_0)\hbar^2/m_\mu e^2 = 256 \text{ fm}.$$

https://doi.org/10.1017/CBO9781139164405.013 Published online by Cambridge University Press

In particular it is energetically highly favourable for muons to displace electrons in atoms.

A muon incident on the D_2–T_2 mixture will lose energy mainly by collisions with the electrons binding the D_2 and T_2 molecules (see Chapter 14), and when it has slowed sufficiently it will break up a molecule and take the place of an electron in either a deuterium or tritium atom. Initially it is likely to be a highly excited state of this muonic atom, but it will quickly cascade down to its ground state. Furthermore, muons initially bound to deuterons in a $(d\mu)$ atom will transfer to tritons in subsequent collisions, since they are more tightly bound in the ground state of a $(t\mu)$ atom by 48 eV (Problem 2.9). The details of these processes are complicated, but they are rapid, and happen in $< 10^{-8}$ s at liquid hydrogen density.

The neutral $(t\mu)$ atom is very small on the scale of a D_2 molecule. It can therefore move almost freely through the electronic cloud of a D_2 molecule to join with a deuteron to form a $(d\mu t)^+$ ion. This ion is a muonic analogue of the hydrogen molecular ion $(H_2)^+$. The process of formation is very rapid compared with other possible competing processes, occurring in $\sim 5 \times 10^{-9}$ s. The reason for this is the existence of a loosely bound (highly excited) state of the $(d\mu t)^+$ ion which, by happenstance, is almost in resonance with an excited vibrational state of the composite $(d\mu t)^+$ ee d molecule. Thus the energy released by the formation of the $(d\mu t)^+$ ion can be transferred and dissipated.

The $(d\mu t)^+$ ion will fall to its ground state, losing energy to electrons. In this ground state the distance between the d and t nuclei is reduced by a factor ~ 200, compared with the distance ~ 1 Å between the hydrogen nuclei of a H_2^+ ion, and hence is ~ 500 fm. Quantum tunnelling through the Coulomb barrier allows the deuterion and triton to interact in $\sim 10^{-12}$ s (see Problem 10.6):

$$\mathrm{d} + \mathrm{t} \rightarrow {}^4_2\mathrm{He} + \mathrm{n} + 17.62\ \mathrm{MeV},$$

as in (10.21).

The nuclear energy released is taken up by the high recoil energies of the α-particle and neutron. The muon is usually freed, to repeat the cycle (Fig. 10.6). However there is a small 'sticking probability' ω_s that the muon is captured by the positively charged α-particle, and may remain bound until it decays. Theoretical estimates give $\omega_s \sim 0.8\%$. Though small, this probability (rather than the mean life of the muon) is the limiting factor in the number of fusions a muon can on average catalyse.

https://doi.org/10.1017/CBO9781139164405.013 Published online by Cambridge University Press

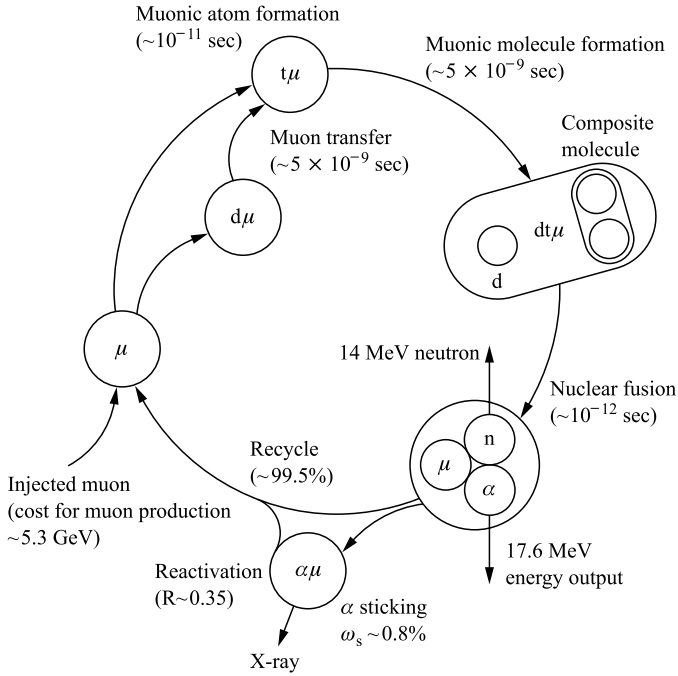


Fig. 10.6 The muon-catalysed fusion cycle: time scales and energies. (Rutherford Appleton Laboratory, ISIS Facility Annual Report 1997–98.)

Experimental figures of up to 200 fusions by a single muon have been reported.

The prospects of muon-catalysed fusion becoming a useful source of power are slight: even 200 fusions yield only 3.5 GeV of fusion energy, which is very much less than the present energy cost of producing the muon.

Problems

10.1(*a*) Assuming that the entire energy output from the Sun is derived from the PPI chain, estimate the flux of neutrinos at the Earth. (Distance of Earth from Sun $\sim 1.5 \times 10^8$ km.)

(*b*) The cross-section for a solar neutrino to interact with a nucleus is $\sim 10^{-20}$ b (cf. Problem 13.3). Show that such a neutrino incident on the Earth is very likely to pass through it unimpeded.

https://doi.org/10.1017/CBO9781139164405.013 Published online by Cambridge University Press

10.2 Why is the hydrogen content of the Earth so much less than that indicated in Table 10.1?

10.3 In the β-decay of ^{8}B, the neutrino takes on average about half of the energy released. Estimate the contribution to the Sun's luminosity per hydrogen atom consumed in the PPIII chain.

10.4 From Fig. 10.1, at the centre of the Sun $k_{\mathrm{B}}T = 1.35$ keV and the mass density of hydrogen is 5.6×10^{4} kg m^{-3}.

(*a*) Using equations (10.5), (10.6) and (10.8) estimate the contribution to the power density ε from the PPI chain. Compare your result with Fig. 10.1(*b*).

(*b*) For the ^{12}C–p reaction of the CNO cycle, $S(0) = 1.4$ keV b. Estimate the mean time it takes for a ^{12}C nucleus at the centre of the Sun to be converted to ^{13}N.

10.5 A deuterium–tritium plasma contains ρ_{d} deuterium and ρ_{d} tritium nuclei per unit volume.

(*a*) Show that to a good approximation $\rho_{\mathrm{d}}(t)$ varies with time as $\mathrm{d}\rho_{\mathrm{d}}/\mathrm{d}t = -\rho_{\mathrm{d}}^{2}\overline{\sigma v}$, where σ is the cross-section for the reaction

$$\mathrm{d} + \mathrm{t} \rightarrow \mathrm{He} + \mathrm{n} + 17.62\ \mathrm{MeV}.$$

(*b*) If the plasma is brought together at time $t = 0$ with $\rho_{\mathrm{d}} = \rho_0$, and confined for a time t_{c} at constant temperature, show that the proportion of the plasma 'burnt up' is

$$\frac{\overline{\sigma v}(\rho_0 t_{\mathrm{c}})}{1 + \overline{\sigma v}(\rho_0 t_{\mathrm{c}})}.$$

(*c*) At $k_{\mathrm{B}}T = 20$ keV, $\overline{\sigma v} = 5 \times 10^{-22}$ m^{3} s^{-1}. What Lawson number $(\rho_0 t_{\mathrm{c}})$ would be required to burn 5% of the fuel?

10.6 Take the Schrödinger equation for the relative motion of a deuteron and triton bound by a muon to be

$$-(\hbar^{2}/2M)\nabla^{2}\psi + V(r)\psi = E\psi$$

where $V(r) = \dfrac{e^{2}}{4\pi\varepsilon_0 r} + Kr^{2}$, $M = \dfrac{m_{\mathrm{d}}m_{\mathrm{t}}}{(m_{\mathrm{d}} + m_{\mathrm{t}})} = 1125\ \mathrm{MeV}/c^{2}$; M is the reduced mass of the system. The term $e^{2}/(4\pi\varepsilon_0 r)$ gives the Coulomb repulsion between the nuclei and the term Kr^{2} models the muon binding.

(*a*) Sketch $V(r)$, and show that it has a minimum at $r = r_0$ where $r_0^{3} = (e^{2}/4\pi\varepsilon_0)/2K$.

(*b*) Show that classically the system can make small oscillations about $r = r_0$ with frequency ω, where

https://doi.org/10.1017/CBO9781139164405.013 Published online by Cambridge University Press

$$\omega^2 = 3(e^2/4\pi\varepsilon_0)/Mr_0^3.$$

(*c*) What is the quantum energy of the system in its ground state, if $r_0 = 500$ fm?

(*d*) Using the formula (6.15), suitably modified, estimate the probability of tunnelling through the Coulomb barrier at this energy.

(*e*) Hence estimate the mean life of the system.

https://doi.org/10.1017/CBO9781139164405.013 Published online by Cambridge University Press